APPLICATION NOTE

Investigate mechanism of action of drugs targeting TPD-43 phosphorylation and aggregation with HTRF based detection assays.

Key features

This Application Note Illustrates how to assess phospho-TDP-43 modulation (Ser 409/410) with HTRF assays combined to the Protein Disaggregation kit in aggregated models.

Abstract

In the field of neuroscience, protein aggregation is a common marker of several neurodegenerative diseases that can be associated with an abnormal or exacerbated phosphorylation status. This application note explains how to reliably and easily assess the modulation of TDP-43 phosphorylation (Ser409/410) despite its various aggregation states in different pathological cellular models by combining the use of the Protein Disaggregation Kit and the HTRF® Phospho-TDP43 Ser409/410 Kit. The comprehensive set of HTRF® data presented here were closely correlated with immunofluorescence imaging results, paving the way to the development of novel drug compounds with potent pharmacological effects against the most prominent hallmarks of TDP-43 proteinopathies.

Introduction

TDP-43 involvement in neurodegenerative diseases

The Trans-Activator Response (TAR) DNA-binding Protein (TDP-43) is a shuttling protein identified to the transport of nucleic acid between nucleus and cytoplasm of cells and participating to the RNA metabolism. Under physiological conditions TDP-43 is a predominantly nuclear protein. Its involvement in neurogenerative disease is well described through hyperphosphorylation, ubiquitination, cleavage of C-terminal fragments, and aggregation leading to neurotoxic effects. Regardless of its localization, phosphorylation of TDP- 43 has been linked to changes in solubility and aggregates formation. The pathological accumulation of phospho-TDP-43 at Serine 409/410 represents a major hallmark of TDP-43 proteinopathies as Frontotemporal lobar degeneration

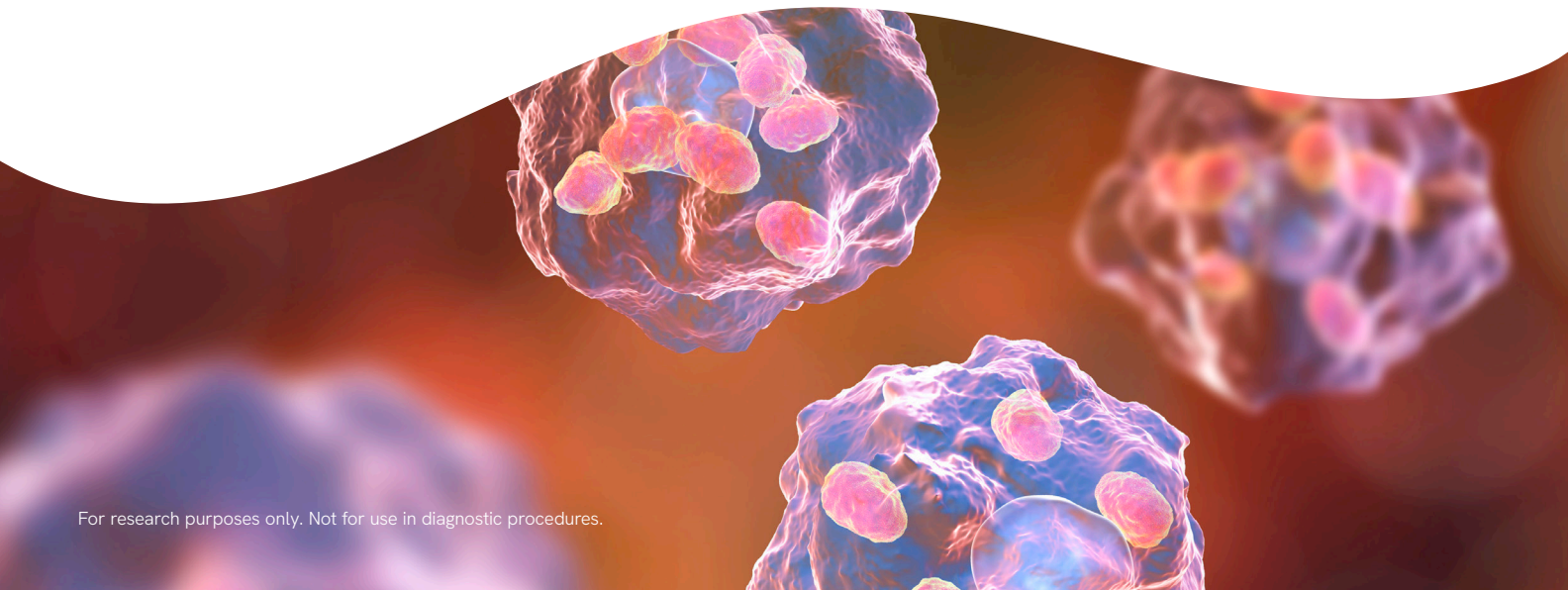

(FTLD) and amyotrophic lateral sclerosis (ALS) but also Alzheimer's disease or Parkinson's disease.

The cleavage of TDP-43 by caspases generates aggregated and hyperphosphorylated C-Terminal Fragments (CTF, 25 and 35 kDa) located in inclusion bodies of some neurodegenerative disorders suggesting an important role of TDP-43 in diseases onset and opening new hopes for the identification of innovative treatments.[4,5]

Indeed, aberrant phosphorylation of C-Terminal TDP-43 is related to disease progression and overexpression of kinases that initially regulated TDP-43 phosphorylation.[3,6,8] Particularly, Casein kinases 1 and 2 (CK-1 and CK-2) were shown to phosphorylate TDP-43 in vitro and it was described that CK-1δ inhibition prevents TDP-43 phosphorylation.[1, 7, 8] Based on different studies, kinases and phosphatases that regulate TDP-43 phosphorylation were identified as potential effective therapies especially for ALS and FTLD.

In this work, we first validated the ability to assess the level of phosphorylation in non-aggregated cellular models, and in TDP-43 aggregated conditions using different compounds modulating TDP-43 signaling pathway (Figure 1). Then we generated different models, characterized by immunofluorescence, mimicking pathological state of TDP-43 to investigate mechanism of action of drugs such as kinase inhibitor to reverse aggregation and /or phosphorylation.

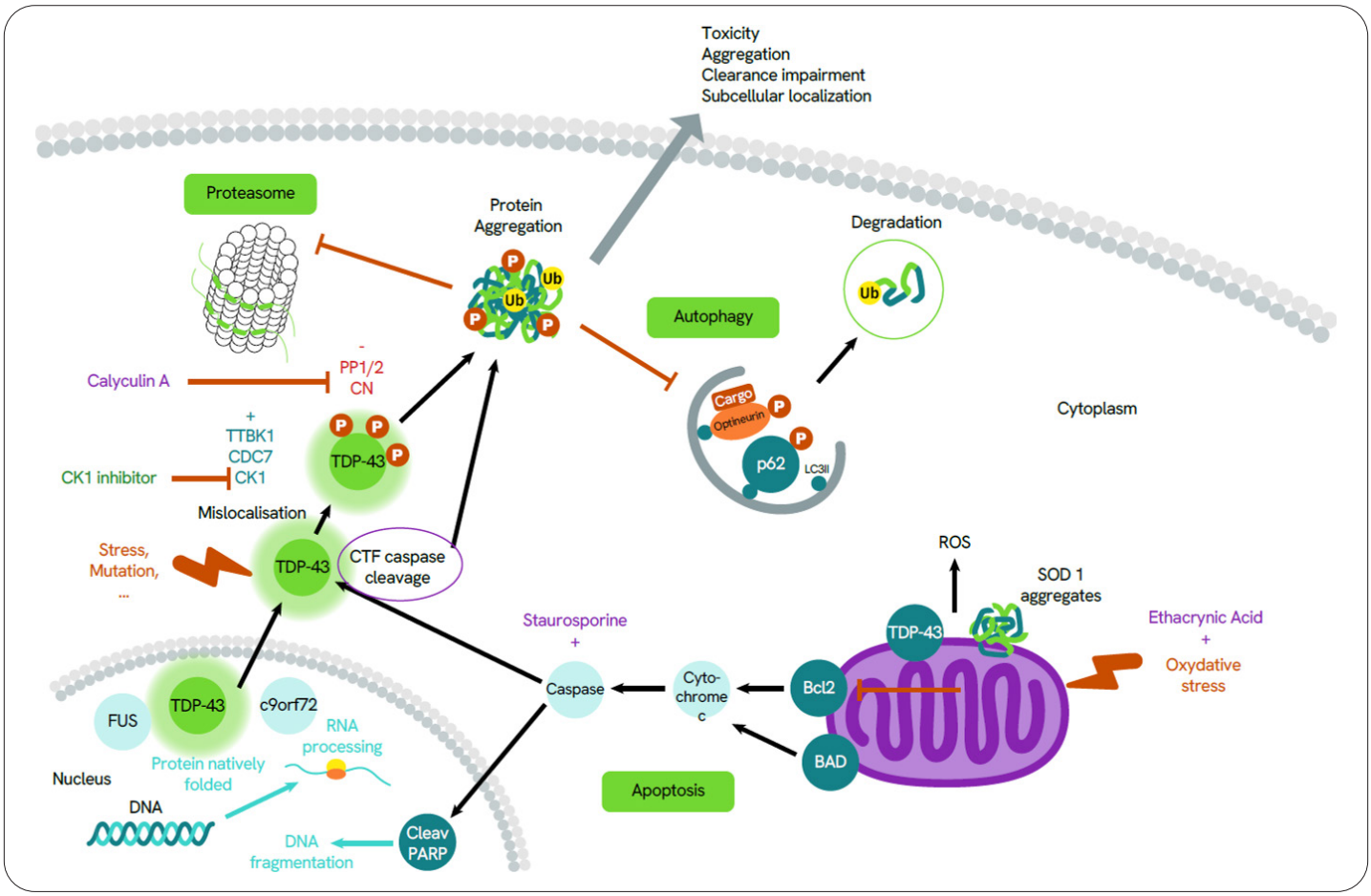

Figure 1: TDP-43 signaling pathway. **Ethacrynic acid** is a glutathione S-transferase inhibitor that increases cellular oxidative stress by depleting glutathione, and it induces TDP-43 C-terminal phosphorylation, insolubilization and C-terminal fragmentation. Calyculin A is a selective inhibitor for PP1/2A, leading to accumulation of phosphorylation of TDP-43. Staurosporine induces activation of caspases leading to the promotion of cleavage of TDP-43 generating C-terminal fragments correlated with aggregates positive to phosphorylation and ubiquitination. CK1 inhibitors were shown to reduce TDP-43 phosphorylation.

Results and discussion

The pathological inclusions in neurodegenerative diseases are composed of TDP-43 which is abnormally phosphorylated and truncated in neurons. Prior to trying to reverse the phosphorylation of TDP-43 in pathological condition of TDP-43 aggregation using a CK1 inhibitor, it was necessary to check the ability to detect the regulation of phosphorylation on S409/410 in different cellular models corresponding to normal conditions or pathological conditions with aggregation.

Detection of TDP-43 S409/410 phosphorylation in non-aggregated and aggregated models

As shown in Figure 4a, a treatment with Staurosporine induces an aggregation of TDP-43 with an aggregated ratio close to 2 which is not observed with a Calyculin A treatment compared to the control condition in HeLa cells. Both treatments increase the phosphorylation level of TDP-43 on S409/410 (Figure 4b). However, to accurately detect this event in aggregated model induced by Staurosporine treatment, it was necessary to perform a disaggregation protocol. Only after disaggregation steps, the expected level of phosphorylation in aggregates is detectable because of better accessibility to epitopes by the detection antibodies. On the other hand, the phosphorylation induced by Calyculin A treatment is detectable in Control condition and similarly after the disaggregation steps because there is no aggregation (Figure 2a).

The reliable detection of the level of phosphorylation is possible in non-aggregated model of TDP-43 without disaggregation and in aggregated models only after disaggregation treatment.

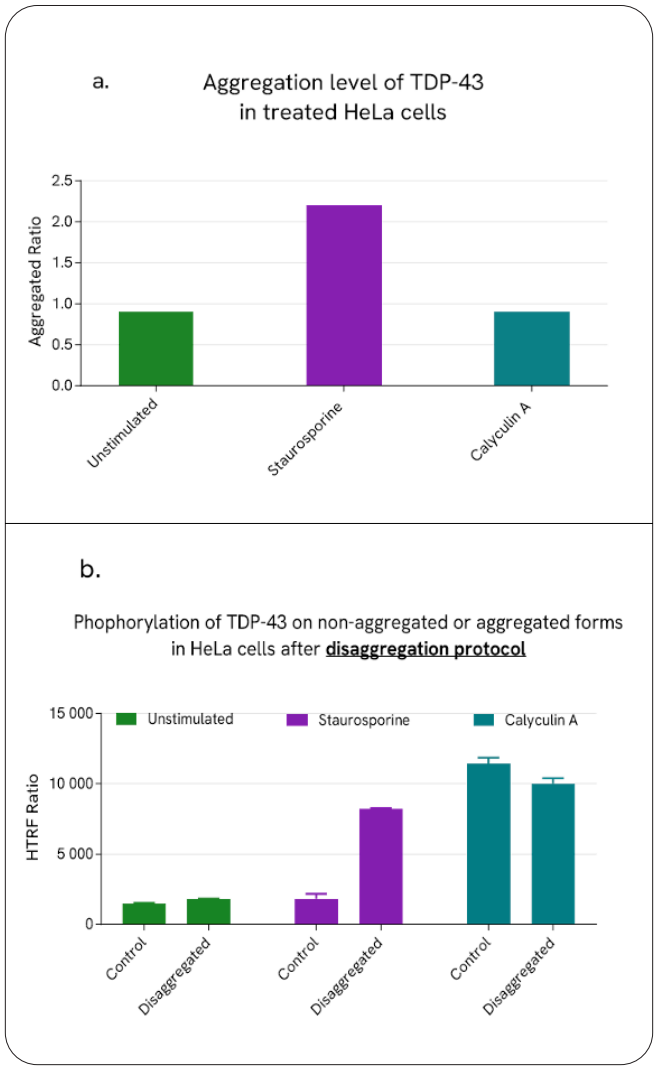

Figure 2: HTRF analysis of aggregation and phosphorylation levels of TDP-43 in HeLa cells upon Staurosporine (1 µM, 6h) and calyculin A (100 nM, 30 min) treatments.

CK1 inhibitor reverses TDP-43 phosphorylation in different non-aggregated models

We next tried to detect the decrease of phosphorylation level of TDP-43 using a CK1 inhibitor in non-aggregated model using Calyculin A treatment on different cell lines such as HeLa cells, SH-SY5Y or Neuro-2a neuroblastomas. The results indicate different phosphorylation patterns depending on the cell line, with a more important level of phosphorylation in Neuro-2a and HeLa cells compared to SH-SY5Y cells after Calyculin A treatment, proving human and mouse compatibility. In all cases, CK1 inhibitor induces a decrease of phosphorylation level proportionally to the concentration used (Figure 3) as described in literature.[6,7] These results showed that the modulation of phosphorylation of TDP-43, namely the increase and decrease via kinase and phosphatase involved in TDP-43 signaling pathway, is detectable using HTRF Phospho TDP-43 S409/410 Detection Kit in non-aggregated TDP-43 cellular models.

CK1 inhibitor reverses phosphorylation in aggregated model detectable after disaggregation

Then, we sought to determine the same event in an aggregated model of TDP-43 using Staurosporine to induce aggregation and phosphorylation as described previously and then inhibits the phosphorylation using CK1 inhibitor. As expected, the results indicate the detection of a phosphorylation increase in this aggregated model after disaggregation, and its inhibition with PF-670462 treatment in a dose-dependent manner until returning to a basal level (Figure 4). It should be noted that cellular toxicity of PF-670462 was checked through Alpha-Tubulin Housekeeping kit and ATPlite™ 1step assay showing no impact at the concentrations used (data not shown here).

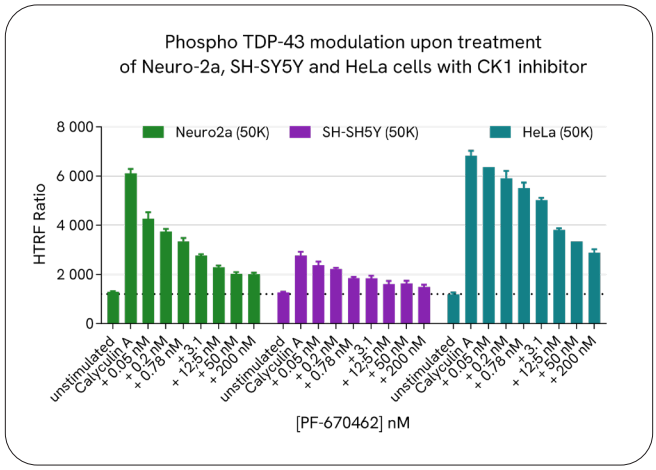

Figure 3: HTRF analysis of phosphorylation levels of TDP-43 in neuro-2a, SH-SY5Y and HeLa cell line upon calyculin A and PF-670462 treatments.

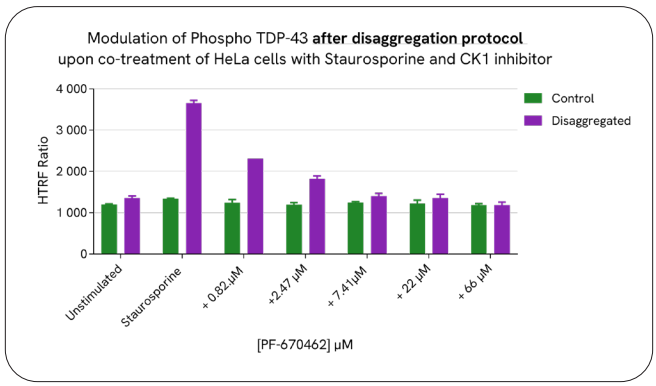

Figure 4: HTRF analysis of phosphorylation levels of TDP-43 in Aggregated HeLa cells upon staurosporine treatment.

These preliminary results pave the way for the use of the Disaggregation Protein kit to accurately detect TDP-43 phosphorylation in aggregated models and enables the study of pathological phosphorylation inhibition.

Detection of phosphorylation in a neuronal model of aggregation

Based on previous results, we tested another compound, Ethacrynic Acid (EA), in a neuronal cellular model (SH-SY5Y cells), known to induce aggregation and phosphorylation of TDP-43, then increasing cellular oxidative stress by depleting glutathione. The aim is to validate a model of TDP-43 aggregation in neuroblastoma cells and to verify the detection of phosphorylation after disaggregation using HTRF assays. The data obtained after Ethacrynic Acid treatment confirm an aggregation of TDP-43 (Figure 5a). In the same way, an increase of phosphorylation level of TDP-43 on S409/410 was detected with an assay window of 2 after disaggregation compared to control condition meaning that the phosphorylation level is associated with the aggregation state. Moreover, without disaggregation the detection of accurate level of phosphorylation is not possible (Figure 5b).

Evaluation of aggregation and phosphorylation level in other aggregated models

Once we demonstrated that it was possible to detect modulations of phosphorylation in aggregated models of TDP-43, we wanted to go further. Inclusions of phospho-TDP-43 in neurodegenerative diseases also contain TDP-43 C-terminal fragments (CTF) particularly 25 kDa CTF. We wanted to assess the level of aggregation through the overexpression of Wild Type TDP-43 corresponding to full length protein and 25 kDa CTF fragments and characterize the phosphorylation level in these aggregates.

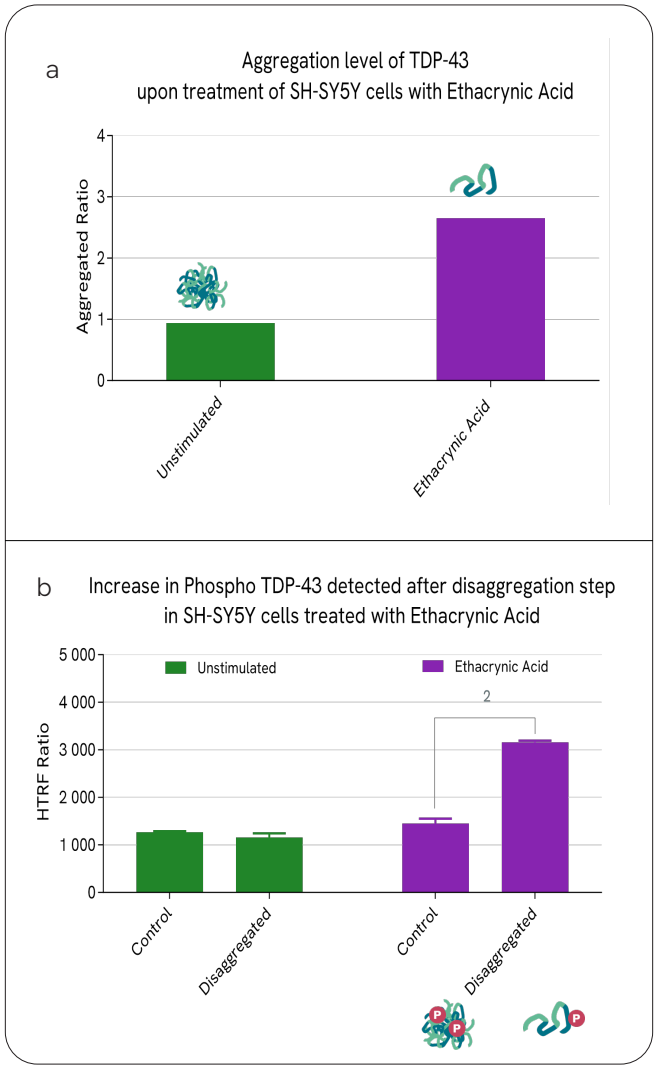

Figure 5: HTRF analysis of aggregation and phosphorylation levels of TDP-43 in SH-SY5Y cells upon ethacrynic acid treatment.

The results indicate that the transient expression of Wild Type TDP-43 and CTF induces an increase of Aggregated ratio of TDP-43 whereas the level of protein expression is similar (data not shown). The expression of TDP-43 CTF gives a higher level of aggregation, more than 2, compared to Wild Type TDP-43 (Figure 6a). Moreover, these aggregations are directly related to phosphorylation level of TDP-43 which is only detected after disaggregation. The data obtained demonstrate that the overexpression of TDP-43 WT in HeLa cells induces an increase of phosphorylation level compared to not transfected cells, mainly in aggregates. The overexpression of C-Terminal Fragment induces a more important phosphorylation by a factor of 2 compared to Wild Type TDP-43 suggesting that C-Terminal Fragment 25 kDa is more prone to hyperphosphorylation and aggregation (Figure 6b).

These two different models of aggregation of TDP-43 can be useful to evaluate drug compounds to treat pathologies associated to aggregation and phosphorylation of TDP-43. Therefore, it appears that in pathological models, TDP-43 Aggregation Kit (#62TDP43PEG/H) and HTRF® Human Phospho-TDP43 Ser409/410 Detection Kit (#64TDPS4PEG/H) combined with the Protein Disaggregation Kit is a suitable platform to screen novel therapeutics against TDP-43 proteinopathies.

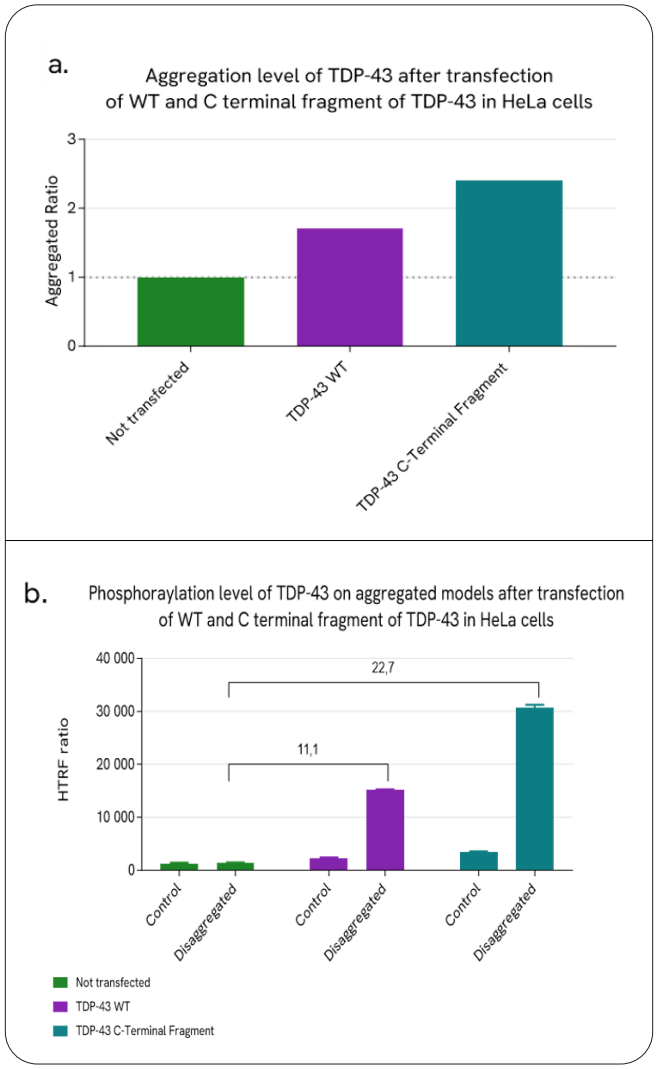

Figure 6: HTRF analysis of aggregation and phosphorylation levels after transfection of TDP-43 Wild Type and TDP-43 C-Terminal Fragments in HeLa cells.

HTRF and immunofluorescence imaging correlation in pathological cell culture models treated with a CK1 inhibitor

Here, we report the effects of a CK-1 inhibitor, PF-670462, on TDP-43 phosphorylation and aggregation levels in HTRF and immunofluorescence imaging.

First, HTRF results indicate that the treatment with PF-670462 reverses the aggregation level after overexpression of Wild Type TDP-43 , down to a basal level corresponding to not transfected cells. Nevertheless, the decrease in the level of aggregation is less significant upon transfection of TDP-43 CTF (Figure 7a).

Likewise, the level of phosphorylation after disaggregation is completely inhibited by PF-670462 after overexpression of Wild Type TDP-43, showing good therapeutic potential in a moderately aggregated model. A similar effect was observed after transfection of TDP-43 CTF but without returning to a basal level of phosphorylation, comparably to the aggregation which also persists (Figure 7b).

Finally, the combination of HTRF data analysis with imaging can give a complete view of aggregation regulation and phosphorylation events in different conditions. To characterize the morphology of these phosphorylated and aggregated overexpressed proteins on different tested conditions, we performed double label immunofluorescence analysis of transfected cells, including the detection of GFP as a tag of transfected TDP-43 and Hoechst to visualize the nucleus.

Immunofluorescence analysis from Operetta revealed a cellular distribution mainly nuclear of Total and GFP-TDP-43 WT (overexpressed). Occasionally, we observed GFP in the cytoplasm, and we attribute this to the overexpression. Phosphorylation of endogenous TDP-43 S409/410 was not seen in control (data not shown) but fluorescence was found after GFP-TDP-43 WT transfection. The phosphorylation is colocalized with GFP-TDP-43 WT in accordance with HTRF showing that the transfection induces phosphorylation of TDP-43 (Figure 8, GFP-TDP-43 WT Control). CK1 treatment in this condition inhibits the phosphorylation level of TDP-43 (Figure 8, GFP-TDP-43 WT Treated), as described in HTRF (Figure 7b).

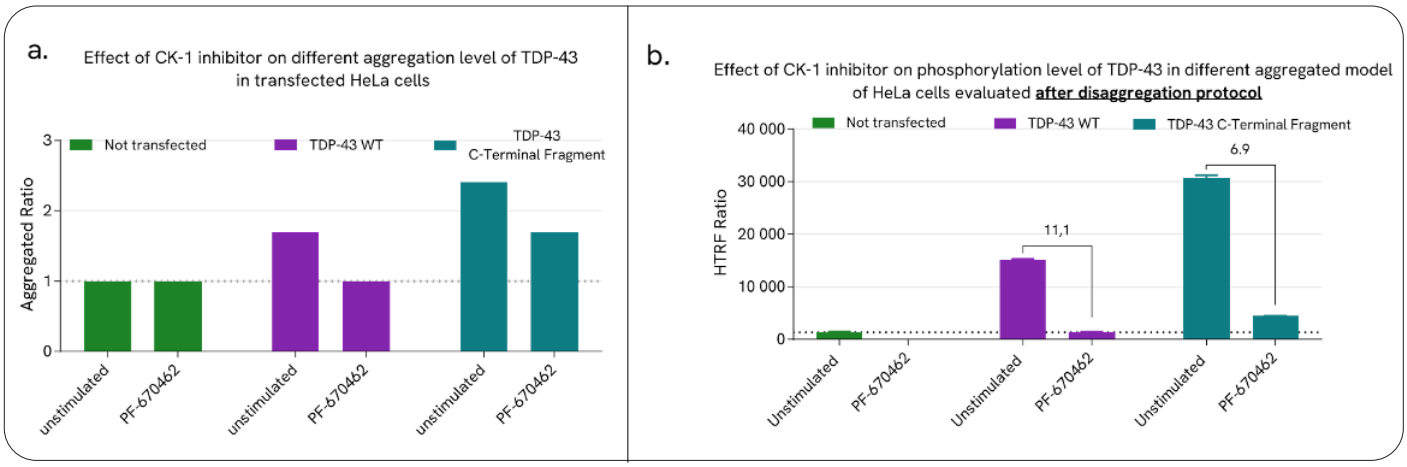

Figure 7: HTRF analysis of aggregation and phosphorylation levels after transfection of Wild Type TDP-43 and TDP-43 C-Terminal Fragments in HeLa cells treated with CK1 inhibitor.

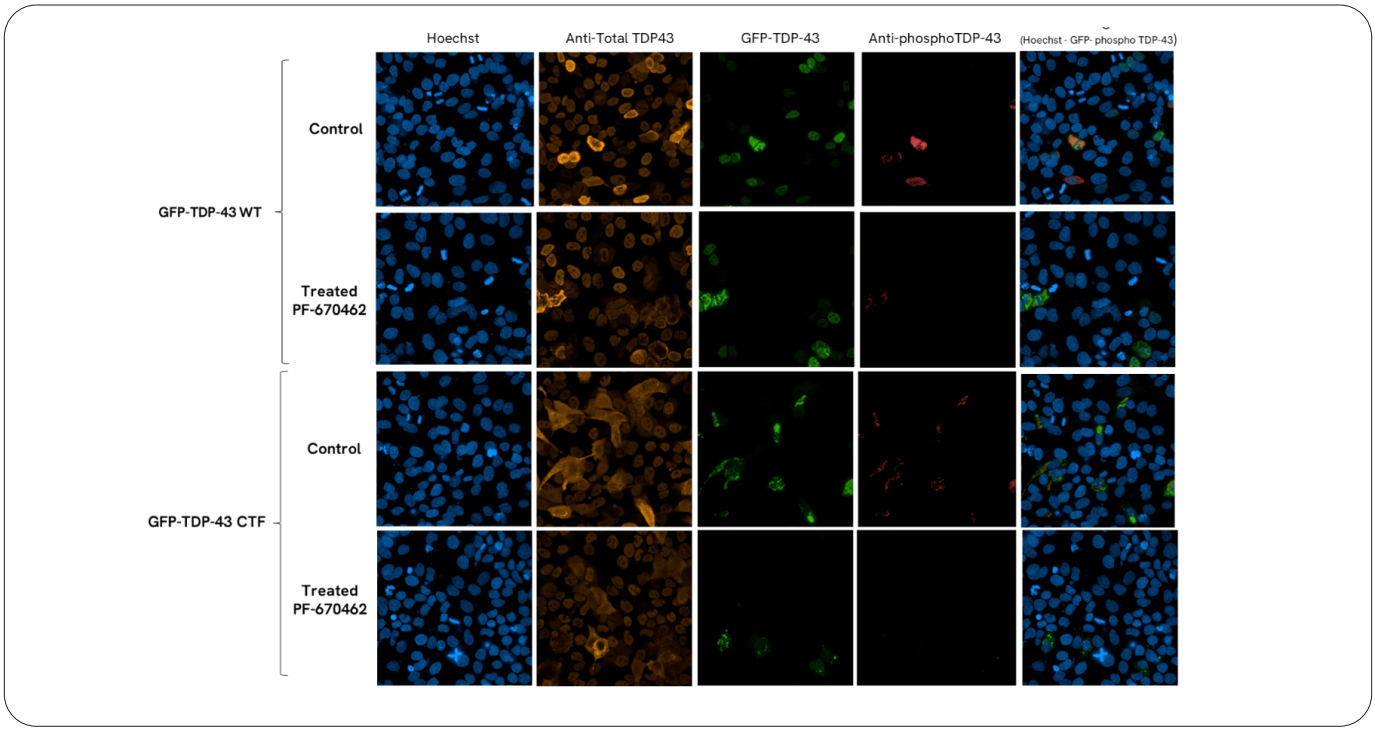

Figure 8: Immunofluorescence analysis of TDP-43 total, GFP-tagged, or phosphorylated on S409/410 in HeLa cells treated with CK1 inhibitor. Hoechst stained nucleus.

In contrast, after transfection of GFP-TDP-43 CTF (25 kDa), data analysis showed a nuclear and cytoplasmic localization of total TDP-43 but mainly cytoplasmic for GFP-TDP-43 CTF, in agreement with the literature (Figure 8, GFP-TDP-43 CTF Control) resulting in the formation of intracellular aggregates (green) positive to phosphorylation of TDP-43 (red). Taken together with the HTRF results, these data indicate a correlation between phosphorylation and overexpression of TDP-43 linked to aggregation. The 25-kDa fragment is believed to be the pathologic species in neurodegenerative diseases. After CK1 inhibitor treatment, we can observe a decrease of phosphorylation level (red) and aggregates presence (green) linked to the overexpression leading to a less cytoplasmic expression of total TDP-43 (Figure 8, GFP-TDP-43 CTF Treated).

All these imaging data validate the cellular models used to recapitulate pathological conditions particularly with C-Terminal Fragments and that the treatment was effective in reducing phosphorylation. In this case, all the HTRF and imaging results show complementary results for screening therapeutic compounds against TDP-43 proteinopathies.

Detection of phosphorylation and aggregation of TDP-43 in human brain lysates

Finally, we wanted to illustrate the ability to detect aggregation and phosphorylation using HTRF assays on brain samples. One control and one with FTLD-TDP- type B positive were tested.[9] Soluble fraction was first evaluated showing a slight detection of TDP-43 without aggregation or phosphorylation detected (data not shown). On the other hand, on insoluble fraction we can detect an aggregation of TDP-43 in FTLD-TDP 43 brain extract only, in agreement with immunoreactive inclusions observed in immunohistology analysis (Figure 11a). In parallel, as expected the phosphorylation of TDP-43 was absent from control, whereas it was detected with a pharmacological window of approximately 2 only after disaggregation steps (Figure 11b). The results suggest that the phosphorylation is localized in the aggregates of TDP-43 in agreement with the literature describing phosphorylation-positive TDP-43 inclusions.[9]

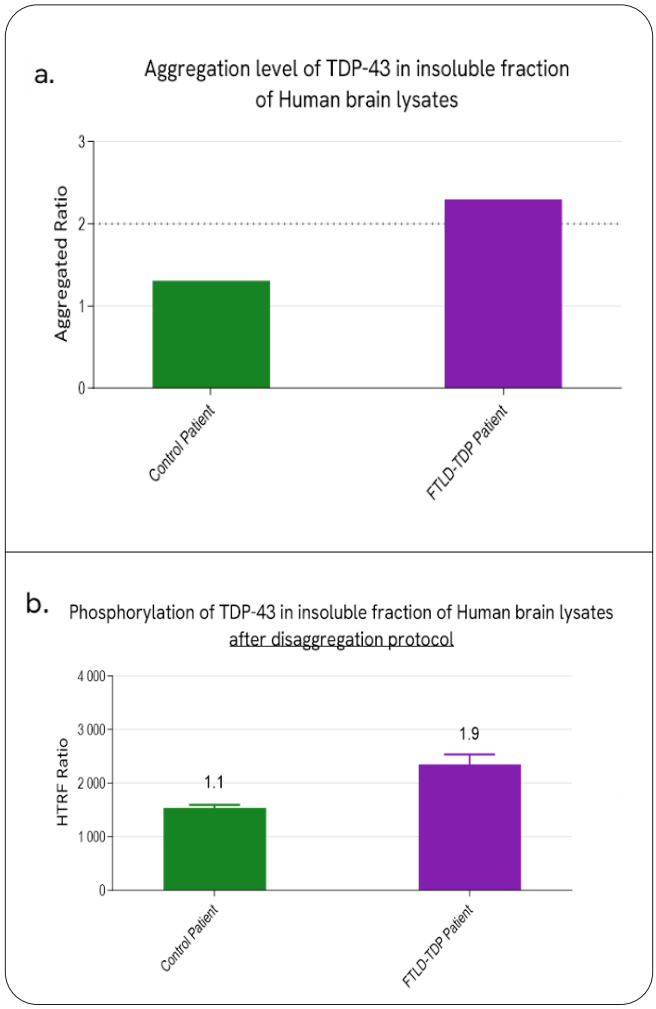

Figure 9: HTRF analysis of aggregation and phosphorylation levels of TDP-43 on Human brain lysates.

It was described that pathological TDP-43 inclusion is resistant to detergents and it is currently complicated at the practical level to separate pathological TDP-43 inclusions from the protein pool in complex tissues. By combining Protein Disaggregation kit and HTRF assays, Revvity offers an innovative easy way to detect TDP-43 phosphorylation in aggregates found in brain lysates, overcoming technical limitations.

Conclusion

Using a panel of TDP-43 non-aggregated and aggregated models, we can accurately assess the modulation of TDP-43 phosphorylation level using the HTRF assays and Protein Disaggregation Kit, demonstrating the need to disaggregate the samples prior to assay detection.

In this context, our data showed differential pathological patterns of TDP-43 proteinopathies, characterized by various level of TDP-43 aggregation and phosphorylation. From this initial characterization, we then used a CK1 inhibitor to inhibit phosphorylation. PF-670462 inhibited the phosphorylation of TDP-43 in aggregated models such as HeLa cells treated with Staurosporine or transfected with TDP-43 C-Terminal fragments. In accordance with literature, the compounds can inhibit the phosphorylation and the level of TDP-43 aggregation.

HTRF technology combined with Protein Disaggregation Kit provides a fast, reliable, and sensitive quantification method for both aggregation and phosphorylation levels in cell or brain lysates, requiring less sample and time to separate the aggregates from the soluble part than conventional Western Blotting techniques. This application note demonstrates that HTRF® and imaging detection gives a complete picture of the compound's mechanism of action on TDP-43 pathological pathway.

Material and Methods

Cell models

HeLa cells from a human cervical carcinoma cell line, were cultured in MEM Alpha medium + glutaMAX TM supplemented with 10% FBS and 1% antibiotics (penicillin/streptomycin) and plated in 96-well white plates half area at 50,000 cells/well, 24h before treatment.

SH-SY5Y cells from the SK-N-SH neuroblastoma cell line, were cultured in DMEM medium + Ham's F12 and glutaMAXTM supplemented with 10% FBS and 1% antibiotics (penicillin/streptomycin) and plated in 96-well white plates half area at 50,000 cells/well, 24h before treatment.

Neuro-2a cells from mouse neuroblastoma cell line, were cultured in EMEM medium supplemented with 10% FBS and 1% antibiotics (penicillin/streptomycin) and plated in 96-well white plates half area at 50,000 cells/well, 24h before treatment.

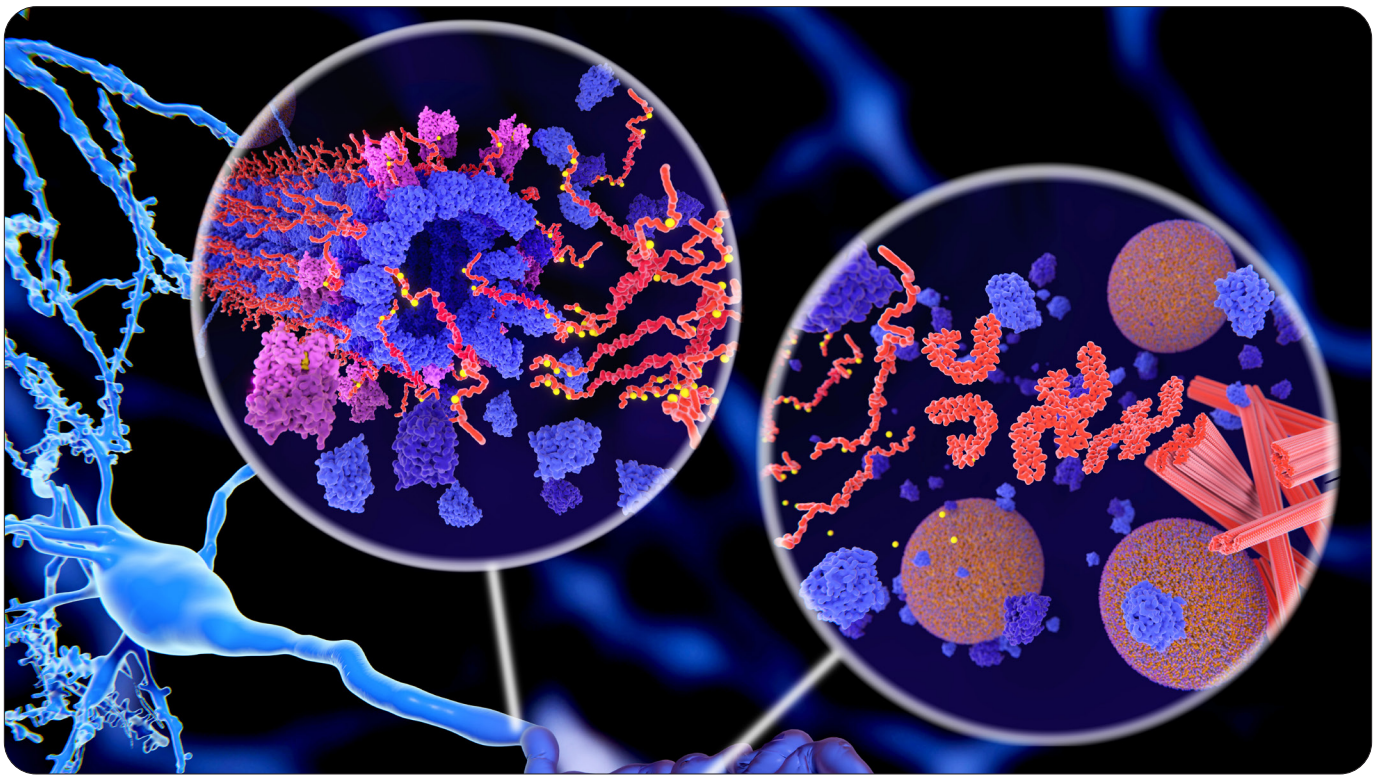

Table 1: Material and reagents.

	Material / Reagent	Supplier	Part Number
Tissue-culture microplates	CulturPlate-96, Black opaque	Revvity	6005660/9
Detection microplates	ProxiPlate-384 Plus, White 384-shallow well	Revvity	6008280/9
Cell Carrier Ultra microplates	PhenoPlate 96-well, black, optically clear flat-bottom	Revvity	6055300/2/8
HTRF® kits	Protein Disaggregation Kit	Revvity	64DAGGRPET/G
	HTRF® TDP-43 aggregation Kit	Revvity	62TDP43PEG/H
	HTRF® Human Phospho-TDP43 Ser409/410 Detection Kit	Revvity	64TDPS4PEG/H
	Alpha-Tubulin Housekeeping	Revvity	64ATUBPEG/H
Luminescence Assay	ATPlite™ 1step Luminescence Assay System	Revvity	6016736/1/9
Cell lines	HeLa cells	ATCC®	CCL-2™
	SH-SY5Y cells	ATCC®	CRL-2266™
	Neuro-2a cells	ATCC®	CCL-131™
Compounds	Staurosporine	Sigma-Aldrich	S4400
	PF-670462	Sigma-Aldrich	SML0795
	Calyculin A	Santa Cruz	sc-24000A
	Ethacrynic Acid	Sigma-Aldrich	SML1083
Transfection	pcDNA 3.1 Human GFP-TDP-43 WT	Revvity	
	pcDNA 3.1 Human GFP-TDP-43 CTF (220-414)	Revvity	11668019
	Lipofectamine 2000TM transfection reagent	ThermoFisher	PVPFA41/2
Immunofluorescence Reagents	PhenoVue Paraformaldehyde, 4% Solution	Revvity	PVPFA41/2
	PhenoVue Permeabilization 0.5% Triton X-100 Solution	Revvity	PVPERM051/2
	PhenoVue Fluor 647 Goat anti-rat Antibody Highly Cross-Adsorbed	Revvity	2GXRB647H1
	PhenoVue Fluor 555 Goat anti-rabbit Antibody Highly Cross-Adsorbed	Revvity	2GXRB555H1
	PhenoVue Hoechst 33342 Nuclear Stain	Revvity	CP71/2
	anti-TDP-43 phospho (Ser409/410) rat antibody, clone 1D3	Biolegend	829901
	TDP43 (D9R3L) Rabbit mAb	CST	89789

Experimental conditions

Cell treatments and sample generation:

To assess phosphorylation and aggregation levels of TDP-43, cells were stimulated with different compounds or transfected to mimic pathological hallmark of aggregation and phosphorylation.

SH-SY5Y cells were dispensed in a CulturPlate-96 (50,000 cells/well) in 50 µL complete culture medium. After 24h of incubation at 37°C - 5% CO2, the cells were treated 5h with 30 µL of increasing concentrations of Ethacrynic Acid prepared in complete culture medium. Following stimulation, 10 µL of supplemented lysis buffer (4X) were added for 30 min at room temperature under gentle shaking.

Neuro-2a, SH-SY5Y and HeLa cells were dispensed in a CulturPlate-96 (50,000 cells/well) in 50 µL complete culture medium. After 24h of incubation at 37°C - 5% CO2, the cells were treated 1h30 with 25 µL of increasing concentrations of CK1 inhibitor or medium only. Then 5 µL of Calyculin A at final concentration of 100 nM prepared in complete culture medium were added. Following stimulation, 10 µL of supplemented lysis buffer (4X) were added for 30 min at room temperature under gentle shaking.

HeLa cells were dispensed in a CulturPlate-96 (50,000 cells/well) in 50 µL complete culture medium. After 24h of incubation at 37°C - 5% CO2, the cells were treated with 30 µL of 100 nM of Calyculin A (10 min) or 1 µM of Staurosporine (6h) alone or with a dose response of PF-670462 prepared in complete culture medium. After treatment, 10 µL of supplemented lysis buffer (4X) were added for 30 min at room temperature under gentle shaking.

Treatment used on cells were stressful so to avoid detachment and loss of cells due to treatment, a suspension cell protocol was implemented. In parallel, a control of viability using ATPlite™1step Luminescence Assay Kit and of cellular content using Alpha-Tubulin Housekeeping HTRF kit were performed. The results presented hereafter correspond to the optimal detection conditions.

Before transfection, HeLa cells were dispensed in a CulturPlate-96 (50,000 cells/well) in 50 µL complete culture medium overnight at 37°C - 5% CO2. For transfection, DNA (pcDNA 3.1 Human GFP-TDP-43 WT, pcDNA 3.1 Human GFP-TDP-43 CTF or pcDNA 3.1 plasmid control) was diluted with LipofectamineTM 2000 in Opti-MEM+ glutaMAXTM medium with a ratio ¼ respectively following supplier recommendation. After culture medium removing, 50 µL of the DNA/Lipofectamine mix was added to cells for 6h at 37°C - 5% CO2. Following transfection, 100 µL of a final concentration of 50 µM of PF-670462 or cell culture medium were added to cells overnight. Finally, after treatment, cell culture medium was removed and 50 µL of supplemented lysis buffer (1X) were added for 30 min at room temperature under gentle shaking or fixed with 50 %L of 4% PFA, 10 min at room temperature.

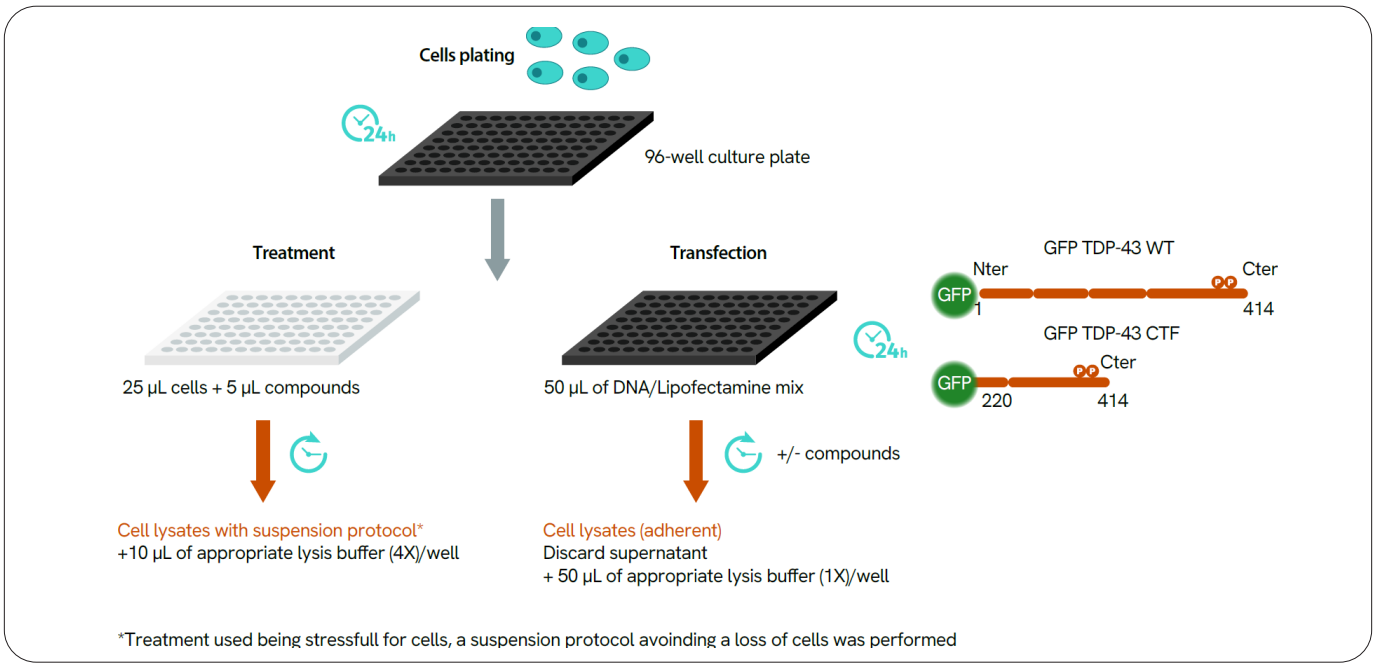

Figure 10: Protocol for obtaining aggregation models.

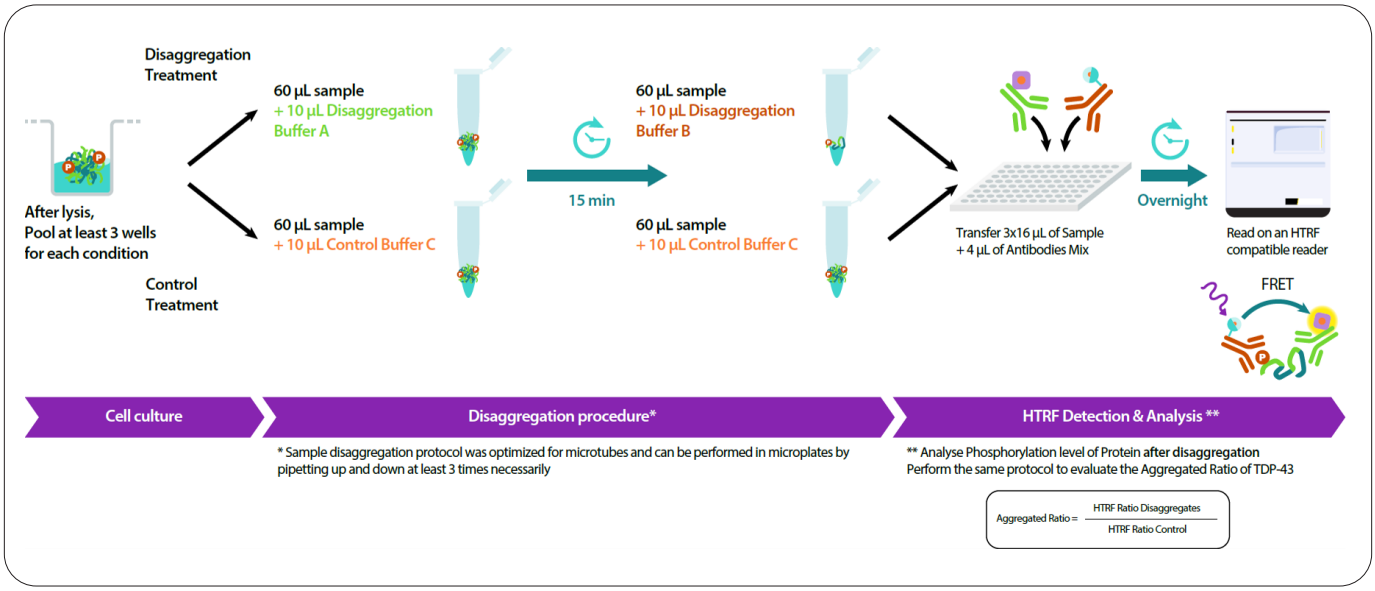

Figure 11: Disaggregation procedure and HTRF detection.

Human brain lysates:

Human biological samples and associated data were obtained from Tissu-Tumorothèque Est (CRB-HCL, Hospices Civils de Lyon Biobank, BB-0033-00046) in accordance with the regulations in force concerning «the use of the elements and products of the human body». Human brain tissue from frontal cortex came from patients with confirmed FTLD-TDP type B, with immunoreactive TDP-43 inclusions or without neuropathological features, defined as Control.[9] Each sample was prepared following the best practices for analyzing brain samples with HTRF phospho assays described in a technical note https://info.perkinelmer.com/technical-note-best-practices-for-analyzing-brain-samples-with-htrf-typ. After lysis and centrifugation (10 min at 1800g) steps, soluble and insoluble fractions were kept and analyzed in HTRF. The insoluble fraction was resuspended in the same volume of supplemented lysis buffer (1X) containing benzonase than soluble part before Disaggregation and HTRF detection.

Disaggregation of samples:

Once the samples are lysed, a rapid disaggregation step is performed on the samples (15 min) to ensure the correct detection of protein phosphorylation in a context of aggregation. After lysis and homogenization by pipetting up and down, at least 3 wells of the same condition were pooled for one HTRF kit (multiply the number of wells proportionally to the number of kits to be tested). Each sample was treated following the kit instructions (Figure 11). Briefly, 2 x 60 µL of each sample were transferred into 2 vials or 2 plate wells and treated with 10 µL of the Disaggregation buffer A or Control detection buffer C.

Following a homogenization by vortexing and 15 min of incubation at room temperature, 10 µL of the Disaggregation buffer A or Control detection buffer C were added. After disaggregation steps, samples are ready for phospho-total HTRF® detection following kit's instructions.

HTRF Detection:

HTRF TDP-43 assays are no-wash sandwich immunoassays based on TR-FRET, where the fluorescent signal intensity is proportional to the TDP-43 concentration in the sample. The detection is achieved using specific antibodies conjugated to donor and acceptor fluorophores. In the case of a phospho TDP-43 S409/410, one of the antibodies specifically recognizes the phosphorylated residues of interest. In aggregate models of TDP-43, detection of TDP-43 phosphorylation events is not measurable because of the lack of phospho epitopes accessibility. The use of Disaggregation Protein Kit ensures a reliable solution to accurately measure protein phosphorylation level.

To perform HTRF assays, 16 µL of sample treated with Disaggregation Protein Kit were transferred into a 384-well low volume white plate, and 4 µL of pre-mixed HTRF detection reagents were added. For the Alpha-Tubulin Housekeeping kit, 4 µL of sample were transferred into the same plate, then 12 µL of kit diluent were added followed by the dispensing of 4 µL of premixed detection antibodies. After incubation according to the manufacturer's instructions, the signal was recorded on an HTRF compatible microplate reader.

To ensure operation within the linear range of each assay, samples were measured neat and diluted. The results presented hereafter correspond to the optimal detection conditions.

HTRF data handling:

The aggregation level of TDP-43 was evaluated using HTRF® the TDP-43 aggregation Kit # 62TDP43PEG.

The measurement of intracellular phospho- TDP-43 S409/410 is a relative quantification where the HTRF signal intensity (HTRF Ratio) is directly proportional to the concentration of the phosphorylated protein in the cell lysate in non-aggregated condition or after disaggregation in aggregate models.

Immunofluorescence and image acquisition:

Transfected HeLa cells were seeded in PhenoPlate 96-well microplates (50,000 cells/well), were fixed with PhenoVue Paraformaldehyde 4% for 10 min at RT, then permeabilized with PhenoVue Permeabilization 0.1% Triton X-100 Solution for 10 min at RT. After 1 h saturation step in PBS 1% BSA at RT, cells were incubated with 1 µg/mL of anti-TDP-43 phospho S409/410 rat antibody and anti-TDP-43 rabbit antibody for overnight at 4°C. After washing step, cells were stained with a solution of PhenoVue Fluor 647 Goat anti-rat highly cross-adsorbed antibody (10 µg/mL), PhenoVue Fluor 555 Goat anti-rabbit highly cross-adsorbed antibody (10 µg/mL) and PhenoVue Hoechst 33342 nuclear stain at (2 µg/mL) for 1h at RT, followed by 3 washes. Finally, images were acquired on Operetta CLS (8 LED) High-Content Screening System in a confocal mode using 63X water objective.

Acknowledgements

We acknowledge the Tissu-Tumorotheque Est (CRB HCL, HCL's biobank) for providing the biological samples used in this study.

References

1. Eck et al., GeroScience (2021) 43:1605–1614. Regulation of TDP-43 phosphorylation in aging and disease.
2. Iguchi et al., Neurobiol Dis. (2012) 45(3):862-70. Oxidative stress induced by glutathione depletion reproduces pathological modifications of TDP-43 linked to TDP-43 proteinopathies.
3. Nonaka et al., Human Molecular Genetics (2009) 18(18): 3353–3364. Truncation and pathogenic mutations facilitate the formation of intracellular aggregates of TDP-43
4. Zhang et al., PNAS (2009) 106(18):7607-12. Aberrant cleavage of TDP-43 enhances aggregation and cellular toxicity.
5. Igaz et al., THE JOURNAL OF BIOLOGICAL CHEMISTRY (2009) 284(13):8516–8524. Expression of TDP-43 C-terminal Fragments in Vitro Recapitulates Pathological Features of TDP-43 Proteinopathies.
6. Brady et al., J Neurochem. (2011) 116(2):248-59. Regulation of TDP-43 aggregation by phosphorylation and p62/SQSTM1.
7. Alquezar et al., Molecular Neurodegeneration (2016) 11:36. Targeting TDP-43 phosphorylation by Casein Kinase-1□ inhibitors: a novel strategy for the treatment of frontotemporal dementia.
8. LAG Da Silva et al., EMBO J. (2022) 41(8):e108443. Disease-linked TDP-43 hyperphosphorylation suppresses TDP-43 condensation and aggregation.
9. Neumann et al., Adv Exp Med Biol. (2021) 1281: 201–217 FTLD-TDP pathological subtypes: clinical and mechanistic significance.

Revvity, Inc.
940 Winter Street
Waltham, MA 02451 USA
www.revvity.com